Electron dynamics in the process of mode switching in gyrotrons

O. Dumbrajs,[1,2] Y. Kominis,[3] and G. S. Nusinovich[4]
[1]*Department of Engineering Physics and Mathematics, Helsinki University of Technology, FIN-02150 Espoo, Finland*
[2]*Institute of Solid State Physics, University of Latvia, Kengaraga Street 8, LV-1063, Riga, Latvia*
[3]*School of Electrical and Computer Engineering, National Technical University of Athens, Association EUROATOM-Hellenic Republic, Zagraphou, GR-15773, Greece*
[4]*Institute for Research in Electronics and Applied Physics, University of Maryland, College Park, Maryland 20742-3511, USA*

(Received 25 September 2008; accepted 25 November 2008; published online 5 January 2009)

The present paper is devoted to the analysis of electron interaction process in the course of gyrotron switching from one mode to another. This analysis is based on the use of the Hamiltonian formalism that allows one to construct Poincaré plots for different instants of switching time. The study is carried out for a 170 GHz, MW-class gyrotron for the International Thermonuclear Experimental Reactor (ITER) [ITER web site: http://www.iter.org]. © *2009 American Institute of Physics*.
[DOI: 10.1063/1.3054555]

I. INTRODUCTION

Gyrotrons are high-power sources of coherent millimeter- and submillimeter-wave radiation capable of delivering MW level of microwave power in continuous-wave regimes (see, e.g., Refs. 1–3). While for a long time the efforts were more or less evenly distributed between the theory (see, e.g., Ref. 4) and experiments, in recent years, the attention of gyrotron developers has been focused primarily on the design of MW-class gyrotrons with the use of available numerical codes, and on gyrotron manufacturing, assembling, and testing. In addition to this mainstream, there are also some continuing efforts aimed at better understanding the physics of electron interaction with microwave fields in gyrotrons. These efforts are not limited by the interaction processes inside gyrotron cavities (see, e.g., Refs. 5–8). In focus are also such processes as excitation of microwave fields by electron beams before the cavity, i.e., in the region between an electron gun and the cavity,[8] as well as a so-called aftercavity interaction. The latter takes place in the region of an up-tapered waveguide where the cyclotron resonance condition can be fulfilled for electrons moving in the decreasing magnetic field and the waves radiated from the cavity region—such waves propagate with the axial wavenumber increasing along the up-taper.[9,10]

One of the issues which still need better explanation is the electron dynamics in the process of gyrotron switching from one mode to another. An example of such switching in the process of voltage rise in a 1.2 MW, 170 GHz European gyrotron which is currently under development for ITER is shown in Fig. 1. This gyrotron is designed for operation at the $TE_{32,09}$ mode, but at a given magnetic field (6.76 T), the voltage rise leads to mode switching from the desired mode to the lower frequency parasitic $TE_{31,09}$ mode before the voltage reaches its nominal value of 80 kV. To have a simulation time not prohibitively long, it was assumed that the voltage rise time from zero to the nominal value is equal to 260 μs. Such a time interval is sufficient for slow enough evolution of gyrotron oscillation parameters in the process of voltage rise.

Below we analyze electron interaction with the fields of the two modes during the time of switching; i.e., from 70 ns up to 74 ns.

II. GENERAL FORMALISM

Our analysis is based on the use of known nonstationary gyrotron equations,[11] which for the case of a weakly tapered external magnetic field can be given as

$$\frac{\partial p}{\partial \varsigma} + i(|p|^2 - 1 + \Delta_B)p = i\sum_s f_s \exp[i(\Delta_s \varsigma + \psi_s)], \tag{1}$$

$$\frac{\partial^2 f_s}{\partial \varsigma^2} - i\frac{\partial f_s}{\partial \tau} + \delta_s f_s = I_s \frac{1}{4\pi^2}\int_0^{2\pi}\int_0^{2\pi} p\, d\vartheta \times \exp[-i(\Delta_s \varsigma + \psi_s)]\, d\phi. \tag{2}$$

Here, p is the complex transverse momentum of the electron

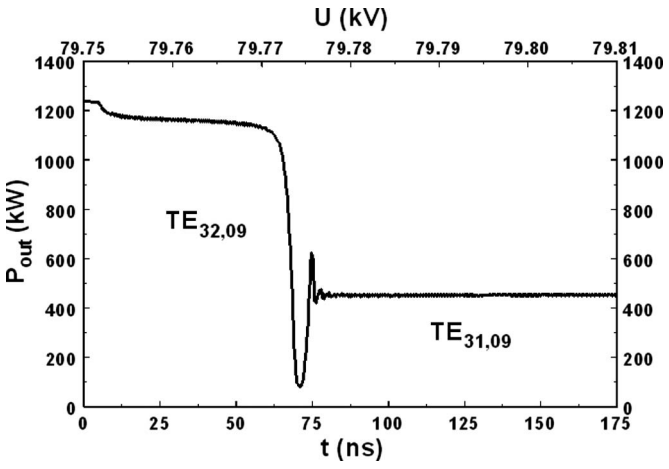

FIG. 1. Switching from the operating $TE_{32,09}$ mode at 170.027 GHz to the parasitic $TE_{31,09}$ mode at 166.985 GHz.

 © 2009 American Institute of Physics

Downloaded 07 Jan 2009 to 147.102.34.127. Redistribution subject to AIP license or copyright; see http://pop.aip.org/pop/copyright.jsp

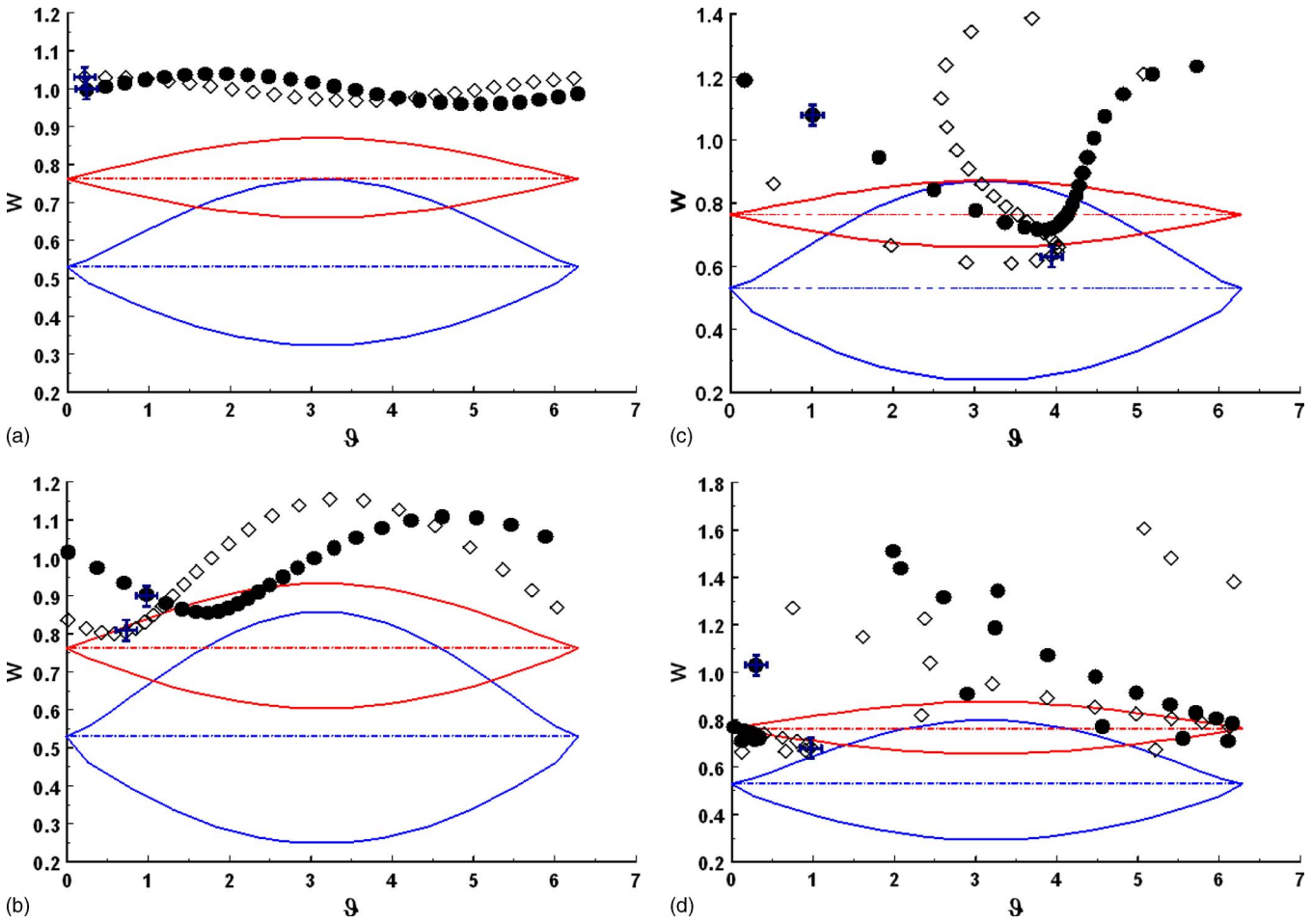

FIG. 2. (Color online) Poincaré plots at four cross sections of the resonator: (a) $\varsigma=\varsigma_{out}/4$, (b) $\varsigma_{out}/2$, (c) $3\varsigma_{out}/4$, and (d) ς_{out} for the time moment $t=70$ ns.

normalized to its initial absolute value, $\zeta=(\beta_\perp^2\omega_{c0}/2\beta_\parallel c)z$ is the dimensionless longitudinal coordinate ($\beta_\parallel=v_\parallel/c$ and $\beta_\perp=v_\perp/c$ are normalized electron velocities, c is the velocity of light, z is the longitudinal coordinate), $(\omega_{c0}/2\pi)$ [GHz] $=28B_0$ [T]$/\gamma_{rel}$ is the initial electron cyclotron frequency defined by the magnetic field $B_0=B(z=0)$ at the resonator entrance (here, $\gamma_{rel}=1+V_b$ [kV]$/511$ is the relativistic factor and V_b is the beam voltage), this frequency is chosen as a carrier one in deriving gyroaveraged equations (1) and (2). Also in Eq. (1) parameter $\Delta_B=(2/\beta_\perp^2)[(\omega_c-\omega_{c0})/\omega_{c0}]$ describes magnetic field tapering along the axis; clearly, the ratio of cyclotron frequencies in this parameter can be replaced by the ratio of magnetic fields. Note that this tapering can be described by an arbitrary function but this variation should be small enough in order to neglect the tapering in all other terms except for the cyclotron resonance mismatch. Then, $\Delta_s=(2/\beta_\perp^2)[(\bar{\omega}_s-\omega_c)/\omega_c]$ is the frequency mismatch for the sth mode, the function $f_s(\varsigma,\tau)$ describes the rf field in resonator which in nonstationary regimes varies in time and along the axis, $\psi_s=8\beta_\parallel^2\beta_\perp^{-4}(\bar{\omega}_s-\omega_c)\omega_c^{-1}\tau+(1\mp m_s)\phi$ is the phase of the mode, m_s and ϕ are the azimuthal index and coordinate, respectively, $\tau=\frac{1}{8}\beta_\perp^4\beta_\parallel^{-2}\omega_c t$ is the dimensionless time, t is time, $\delta_s=8\beta_\parallel^2\beta_\perp^{-4}[\varpi_s-\omega_{cut,s}(\zeta)]\omega_c^{-1}$ describes variation of the cutoff frequency $\omega_{cut,s}(\zeta)$ along the resonator axis, $\bar{\omega}_s$ is the cutoff frequency at the exit from the resonator. Lastly, in the right-hand side of (2), I_s is the dimensionless current which includes the rf field and electron beam coupling:

$$I_s=9.4\times10^{-4}I_b\,[\mathrm{A}]\beta_\parallel\beta_\perp^{-6}\frac{J_{m_s\pm1}^2[(2\pi/\lambda_s)R_{el}]}{\gamma_{rel}(\nu_s^2-m_s^2)J_{m_s}^2(\nu_s)}. \tag{3}$$

In Eq. (3), λ_s is the wavelength, R_{el} is the electron beam radius, and ν_s is the mode eigenvalue. The subscript s refers to the sth mode.

Equation (1) has to be supplemented by the boundary condition $p(0)=\exp(i\theta_0)$, $0\leqslant\theta_0<2\pi$, while Eq. (2) should be supplemented by both initial and boundary conditions. The initial condition can be given as $f(\zeta,0)=f_0(\zeta)$. where $f_0(\varsigma)$ is rf field profile obtained in the cold-cavity approximation. The boundary condition can be written as usual:

$$f_s(\varsigma_{out},\tau)=\frac{i}{k}\left.\frac{\partial f_s(\varsigma,\tau)}{\partial\varsigma}\right|_{\varsigma=\varsigma_{out}}, \tag{4}$$

where $k_s=2c\beta_\parallel\beta_\perp^{-2}\omega_c^{-1}[\bar{\omega}_s^2/c^2-\nu^2(\varsigma)/R_{cav}^2(\varsigma)]^{1/2}$ is the dimensionless axial wave number and R_{cav} is the cavity radius.

It is convenient to perform further analysis on the basis of the Hamiltonian formalism that allows one to construct

Downloaded 07 Jan 2009 to 147.102.34.127. Redistribution subject to AIP license or copyright; see http://pop.aip.org/pop/copyright.jsp

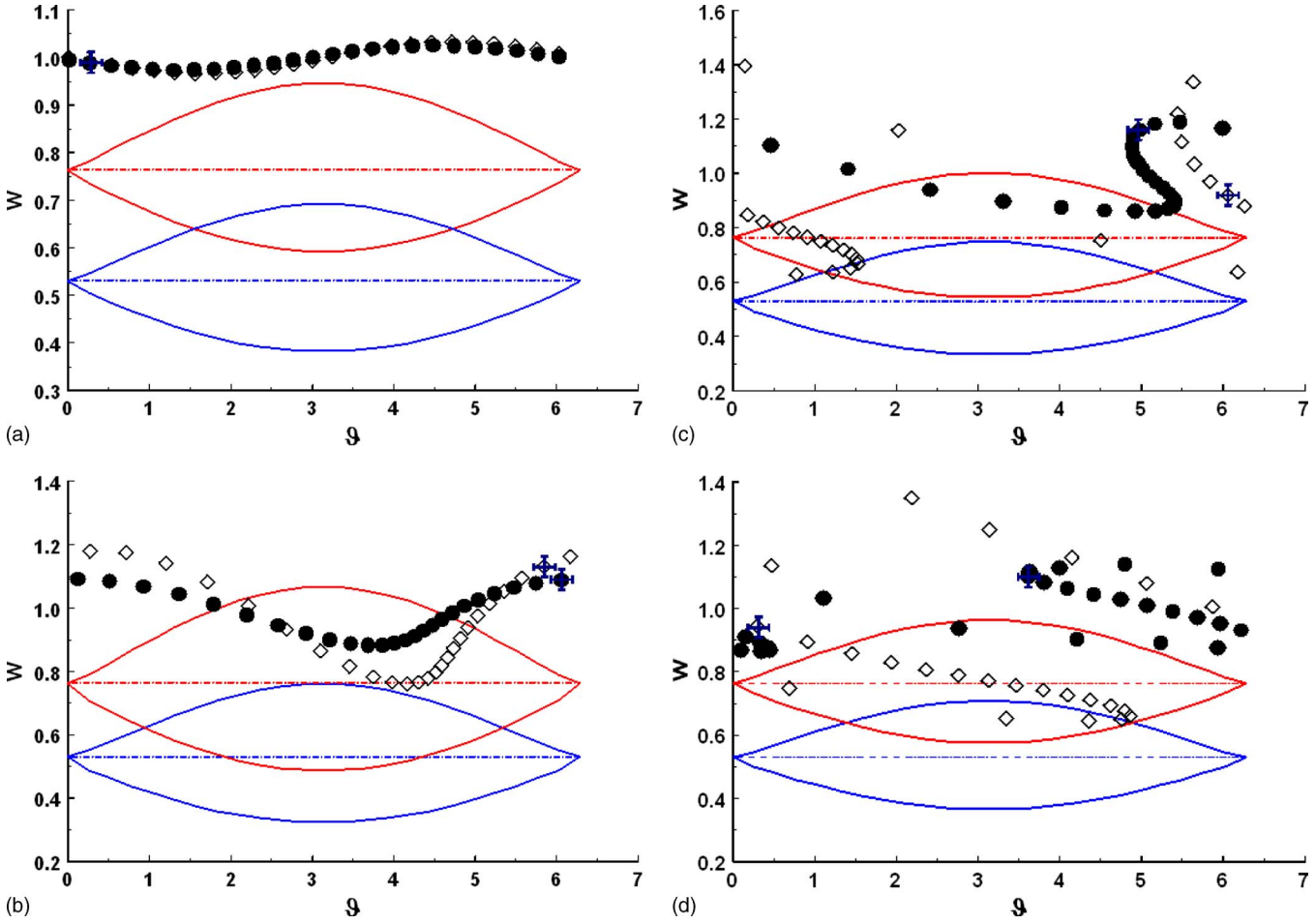

FIG. 3. (Color online) Poincaré plots at four cross sections of the resonator: (a) $\varsigma=\varsigma_{out}/4$, (b) $\varsigma_{out}/2$, (c) $3\varsigma_{out}/4$, and (d) ς_{out} for the time moment $t=72$ ns.

Poincaré plots for different instants of switching time. The latter allow for studying the inhomogeneous structure of the phase space of the respective system, describing electron dynamics. In our case, the phase space has three dimensions corresponding to a nonautonomous system with one degree of freedom. The inhomogeneity of the phase space is a result of the presence of regions corresponding to resonant interactions between the electrons and the rf modes of the cavity. Each one of these resonances is characterized by its center and width in the two-dimensional Poincaré plot (surface of section) of the system. The position of the center is determined by the resonance condition between the electron cyclotron frequency and the frequency of the corresponding rf mode, while the width depends on the amplitude of the rf mode and it is measured at the separatrix (cat's eye) of the resonance. The latter separates two regions of qualitatively different electron motion in the phase space: Inside the separatrix, phase trapping by the rf mode occurs, while untrapped motion takes place outside. Therefore, the relative position of a set of initial conditions, corresponding to an electron beam, with respect to the separatrix of a resonance provides information for the actual interaction of the electron beam with the respective rf mode. This is particularly useful in the case where more than one mode is present, such as in the process of mode switching, and allows for distinguishing the mode with which the electron beam actually interacts mostly. Complex electron dynamics in the presence of two modes have been analyzed in the context of the Hamiltonian formalism in gyrotron resonators in Ref. 6 and somewhat earlier[12] in relativistic gyrotraveling wave devices. The equation for electron motion in a single-mode case can be rewritten[7] in action-angle variables with the Hamiltonian

$$H(w,\theta)=\frac{w^2}{4}-w_r\frac{w}{2}+\sqrt{w}\,\mathrm{Im}(e^{i\theta}f), \tag{5}$$

where $w=|p|^2$, $w_r=1-\Delta$, and $\theta=\arcsin(\mathrm{Re}\,p/\sqrt{w})$. From $H(w,\theta)=H(w_r,0)$, a transcendental equation for the separatrix follows:

$$w=w_r\pm 2\sqrt{\sqrt{w_r}\,\mathrm{Im}\,f-\sqrt{w}\,\mathrm{Im}(e^{i\theta}f)}. \tag{6}$$

III. RESULTS

Simulations were done for the following set of gyrotron operating parameters: $B=6.76$ T, $I_b=42$ A, $R_{el}=9.50$ mm, and $\alpha=1.3$ at $U_b=79$ kV. In solving Eqs. (1) and (2), we used 25 electrons with different entrance phases ϑ and seven groups of electrons with different azimuthal coordinates of

Downloaded 07 Jan 2009 to 147.102.34.127. Redistribution subject to AIP license or copyright; see http://pop.aip.org/pop/copyright.jsp

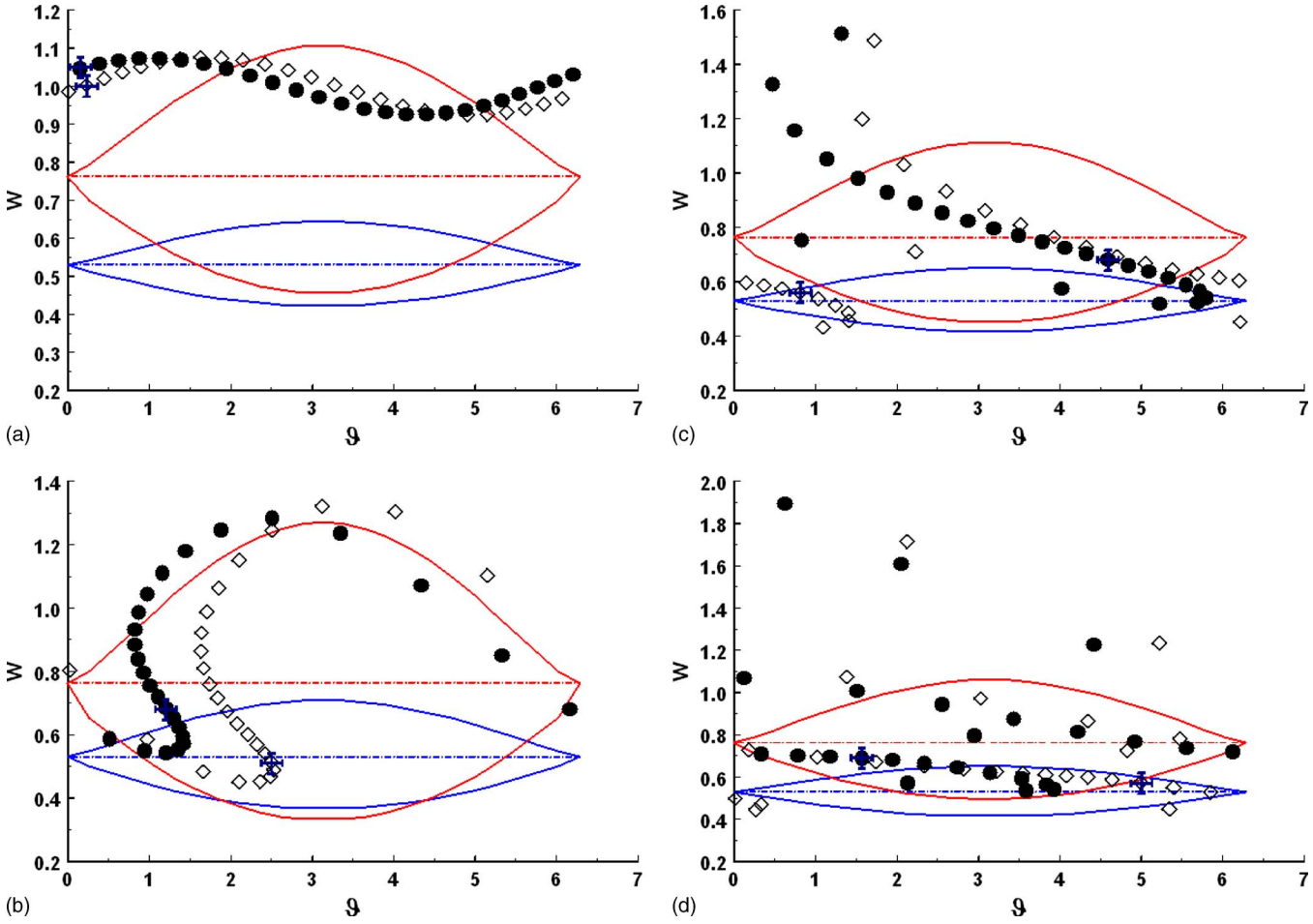

FIG. 4. (Color online) Poincaré plots at four cross sections of the resonator: (a) $\varsigma=\varsigma_{out}/4$, (b) $\varsigma_{out}/2$, (c) $3\varsigma_{out}/4$, and (d) ς_{out} for the time moment $t=74$ ns.

guiding centers ϕ uniformly distributed between 0 and 2π. In Figs. 2–4 we show Poincaré plots at four cross sections of the resonator and three time moments; it is shown electron distribution for electrons having two azimuthal angles of guiding centers: $\phi=2\pi/7$ (black dots) and $\phi=2\pi(4/7)$ (empty diamonds). Crosses mark the electron number one, whose entrance phase is $\vartheta=2\pi/25$. Here the lower cat's eye shows the separatrix of the operating mode and the upper cat's eye shows the separatrix of the parasitic mode.

In Fig. 5, absolute values of axial profiles of both modes for different instants of time are shown. A clear switching from the operating $TE_{32,09}$ mode to the parasitic $TE_{31,09}$ mode is seen. The difference in axial structures of modes shown in Fig. 5 (these structures also vary in time) results in the difference in the height of separatrices shown in Fig. 2 for the same instants of time in different cross sections.

Returning back to Fig. 2, it should be noted that electrons with different azimuthal coordinates of guiding centers exhibit different dynamics in the process of mode switching. This can be considered as a specific feature of the electron interaction with the fields of more than one mode. In the case of single-mode operation, electrons with different azimuthal coordinates of guiding centers exhibit the same behavior in the phase space. However, in the process of mode switching, where two modes are present, electron dynamics depends on the azimuthal coordinate of the guiding center. This can be explained by the fact that the phase difference of these modes is azimuthally dependent. This conclusion can be illustrated by the right figure in the second row in Fig. 2 showing electron distribution at the exit for $t=72$ ns; here, the lowest value of w for black dots is larger than 0.8, while a corresponding minimal value of w for empty diamonds is about 0.5.

IV. CONCLUSIONS

When the guiding magnetic field is chosen properly, the voltage rise results, first, in fulfillment of self-excitation conditions for the operating $TE_{32,09}$ mode; then, at higher voltages, it operates with a high efficiency (possibly, in the region of hard self-excitation). In this regime, the difference between the frequency of this mode and the electron cyclotron frequency is rather large. For the parasitic $TE_{31,09}$ mode with a lower frequency this difference is smaller. Therefore, electrons, which enter the interaction region with the initial value of w equal to unity, in the process of their deceleration by the $TE_{32,09}$ mode first enter the region occupied by the separatrix of the $TE_{31,09}$ mode (red) and, hence, interact with

Downloaded 07 Jan 2009 to 147.102.34.127. Redistribution subject to AIP license or copyright; see http://pop.aip.org/pop/copyright.jsp

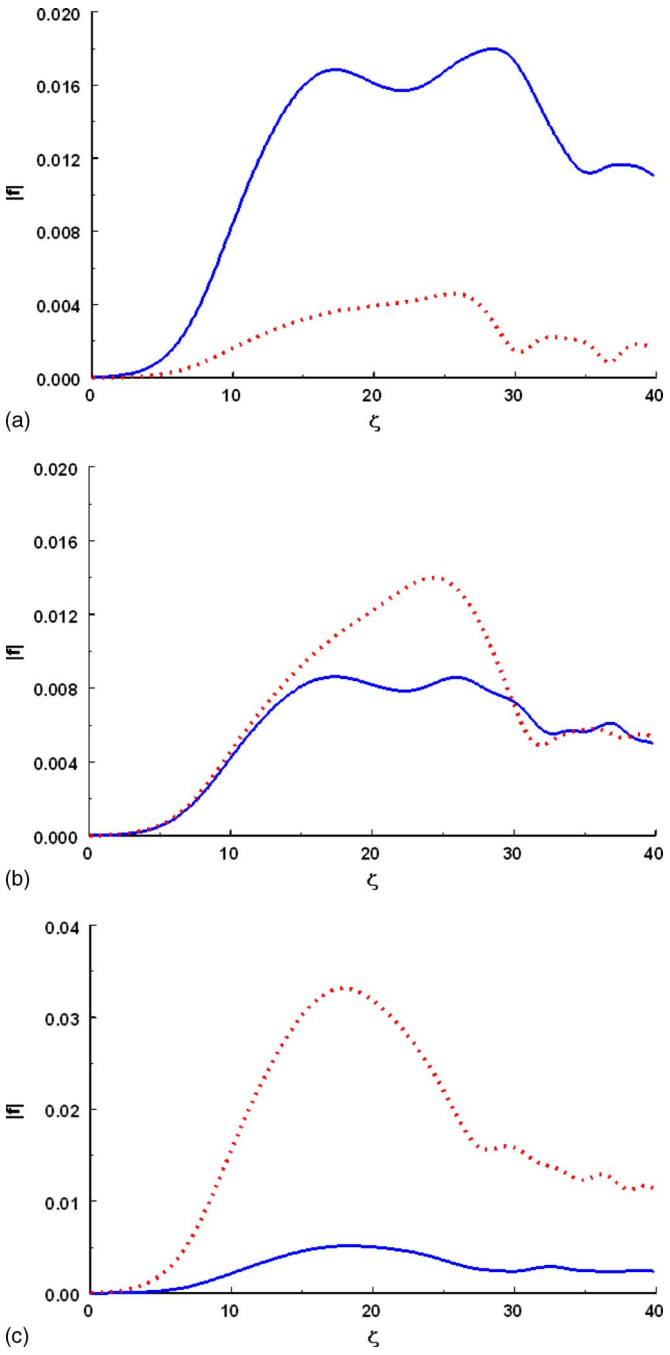

FIG. 5. (Color online) Absolute values of axial profiles of both modes (solid-blue $TE_{32,09}$ and dashed-red $TE_{31,09}$ for the three time moments: (a) $t=70$, (b) 72, and (c) 74 ns.

it in spite of the presence of the $TE_{32,09}$ mode. This gives the preference to the $TE_{31,09}$ mode and so it starts to grow.

Growth of the $TE_{31,09}$ mode is accompanied by significant disturbances in the electron distribution in the phase space. Therefore, when electrons enter the region occupied by the separatrix of the $TE_{32,09}$ mode (blue), they have much less free energy to be transformed to this mode radiation. Thus, the $TE_{32,09}$ mode begins to decay.

It is shown that the electron dynamic in the process of simultaneous interaction with two modes depends on the azimuthal coordinate of electron guiding centers. Correspondingly, the kinetic energy in a spent electron beam at the exit from the interaction space is azimuthally dependent. When the switching process is rather slow, this azimuthal nonuniformity in the energy of spent electrons can be important for collector operation.

ACKNOWLEDGMENTS

The work of O.D. is supported by Association Euratom—TEKES, the work of Y.K. by the European Fusion Programme (EURATOM) and the Greek Secretariat of Research and Technology, and the work of G.S.N. by the Office of Fusion Energy of the U.S. Department of Energy.

[1] K. L. Felch, B. G. Danly, H. R. Jory, K. E. Kresischer, W. Lawson, B. Levush, and R. J. Temkin, Proc. IEEE **87**, 752 (1999).
[2] M. Thumm, Plasma Phys. Controlled Fusion **45**, A143 (2003).
[3] K. Sakamoto, Fusion Sci. Technol. **52**, 145 (2007).
[4] K. R. Chu, Rev. Mod. Phys. **76**, 489 (2004).
[5] G. S. Nusinovich, R. Ngogang, T. M. Antonsen, Jr., and V. L. Granatstein, Phys. Rev. Lett. **93**, 055101 (2004).
[6] Y. Kominis, O. Dumbrajs, K. A. Avramides, K. Hizanidis, and J. L. Vomvoridis, Phys. Plasmas **12**, 113102 (2005).
[7] O. Dumbrajs, Y. Kominis, K. A. Avramides, K. Hizanidis, and J. L. Vomvoridis, IEEE Trans. Plasma Sci. **34**, 673 (2006).
[8] K. Sakamoto, A. Kasugai, K. Takahashi, R. Minami, N. Kobayashi, and K. Kajiwara, Nat. Phys. **3**, 411 (2007).
[9] V. E. Zapevalov and M. A. Moiseev, Radiophys. Quantum Electron. **47**, 520 (2004).
[10] E. M. Choi, M. A. Shapiro, J. R. Sirigiri, and R. J. Temkin, Phys. Plasmas **14**, 093302 (2007).
[11] N. A. Zavolsky, G. S. Nusinovich, and A. G. Pavelyev, in *Gyrotrons*, a book of collected papers (Institute of Applied Physics, Academy of Sciences of the USSR, Gorky, USSR, 1989), p. 84.
[12] P. Latham and G. S. Nusinovich, Phys. Plasmas **2**, 3494 (1995).

Downloaded 07 Jan 2009 to 147.102.34.127. Redistribution subject to AIP license or copyright; see http://pop.aip.org/pop/copyright.jsp